



Universiteit  
Leiden  
The Netherlands

## Superlattices in van der Waals materials: a low-energy electron microscopy study

Jong, T.A. de

### Citation

Jong, T. A. de. (2022, November 3). *Superlattices in van der Waals materials: a low-energy electron microscopy study*. *Casimir PhD Series*. Retrieved from <https://hdl.handle.net/1887/3485753>

Version: Publisher's Version

License: [Licence agreement concerning inclusion of doctoral thesis in the Institutional Repository of the University of Leiden](#)

Downloaded from: <https://hdl.handle.net/1887/3485753>

**Note:** To cite this publication please use the final published version (if applicable).

# 1

## INTRODUCTION

Life in general and science in particular are most interesting at boundaries, on edges and at frontiers. Frontiers of human knowledge, where the unknown meets the known, but also boundaries between different systems. In condensed matter different types of such boundaries exist: between different phases of matter (e.g. a liquid–gas interface), between matter and vacuum (mostly studied by surface science), and between different condensed matter systems. The challenge in studying this last type of system has traditionally been to create an atomically clean interface between the two material systems, and has been served by the art of epitaxy: the deposition of layers of a material on the surface of a second system in an inert atmosphere. By ensuring the interface is atomically clean, it becomes possible to study the interaction between the two systems, how they bond and, of particular interest in this work, how their different lattices reconcile.

The boundary between two three-dimensional systems is a two-dimensional plane. As the dimensionality plays a large role in the description of electrons in materials, creating a truly two-dimensional electronic system has been a goal in experimental physics. An important early example are the gallium arsenide / aluminium gallium arsenide epitaxial interfaces, where a two-dimensional electron gas forms. Aside from physically interesting phenomena, e.g. the Hofstadter butterfly [1], this system also forms the basis of high-frequency field effect transistors.

The true start of the field now known as two-dimensional materials came in 2004, when Konstantin Novoselov and Andre Geim et al. realized the first two-dimensional material, showing that it was possible to thin down layered materials to a thickness of only a single atom using simple scotch tape [2]. As it turned out, the carbon atoms in graphite form layers that are strongly bonded by covalent bonds within a layer, but the layers are only held together by much weaker van der Waals forces (as visible in the schematic representation of graphite in Figure 1.1a). Therefore, tape sticks more strongly to the layers than the layers stick to each other, making it possible to peel layers of graphite from a crystal using tape. By sticking a new tape to the material on the tape, the peeled off layer can be split again, and again, until a single layer of carbon atoms in a hexagonal arrangement remains: graphene. This process to obtain atomically thin layers is called exfoliation.

The advent of exfoliation as a technique for the production of two-dimensional materials has started extended studies of atomically thin layers. Most notably, the electronic behavior changes as these materials become truly two-dimensional as no copies of the same electron orbital exist along the out-of-plane direction, leading to extraordinary properties.

After the original exfoliation of graphene, a larger assortment of materials has been added to the collection of so-called van der Waals materials. This includes the insulating material hexagonal boron nitride (hBN, Figure 1.1b), with the same structure as graphene, but consisting of alternating boron and nitrogen atoms, and the transition metal dichalcogenides (TMDs, Figure 1.1c,d), where the van der Waals layer consists of a layer of trigonally arranged transition metal atoms (molybdenum, tantalum, niobium, tungsten, etc.) sandwiched between two layers of chalcogens (sulfur, selenium or tellurium<sup>1</sup>). The set of all possible TMDs spans a wide range of properties: from semi-

<sup>1</sup>Aside from obvious reasons to not use these elements, polonium and livermorium tend to be too metallic in character to form TMDs [3]

conductor to metal, magnetic, and superconductor, often combining several properties depending on the temperature.

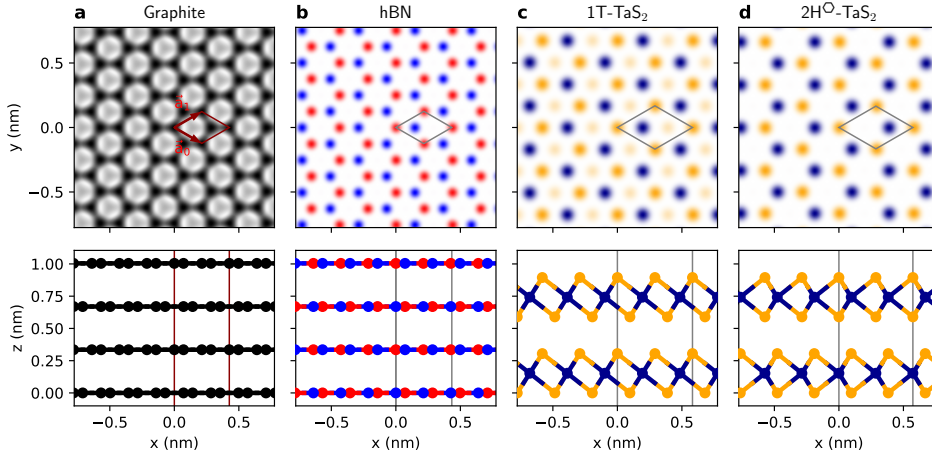


**Figure 1.1: Van der Waals materials.** Top views and side views along the so-called arm chair direction of different van der Waals materials: graphite, the ‘mother material’ of graphene, its insulating sibling hexagonal boron nitride and the TMD TaS<sub>2</sub>. In TMDs, different polytypes (layer arrangements) exist. Two of the stable polytypes for TaS<sub>2</sub> are shown: 1T and 2H<sup>○</sup> (For more details about polytypes, see Section 8.1.2).

In addition to the study of intrinsic properties of these 2D materials, exfoliation has led to a new way of studying matter–matter boundaries: by transferring subsequent van der Waals layers via exfoliation, so-called **heterostacks** of different layers with (areas of) an atomically clean interface between the subsequent layers can be created. In this way different electronic properties can be combined, used adjacent to each other, or even hybridized to create new properties.

The parameter space is enormous: in addition to the possibility to combine any pair of van der Waals materials, independent of the existence of conventional epitaxial growth procedures<sup>2</sup>, the twist angle between subsequent layers enters the picture as a tunable parameter. This means that even interfaces between two layers of the *same* material can become interesting: a non-zero twist angle between the materials leads to a moiré pattern with its own larger geometry (the ‘super’ lattice), with significant influences on the electronic structure. Famously, this has led to the observation of superconductivity in twisted bilayer graphene (TBG), which forms a flat electronic band when the two layers are stacked at a ‘magic’ twist angle of approximately one degree [4, 5].

## 1.1 GROWING 2D MATERIALS

Maybe somewhat ironically, the interest in two-dimensional materials has also renewed the interest in traditional epitaxy: while exfoliation is an excellent platform to study 2D

<sup>2</sup>Although not all materials exfoliate to single layers with the same ease. There is no such thing as a free lunch.

materials, the process does not scale to industrial applications. Therefore, epitaxy, i.e. growing a 2D material on the surface of a 3D substrate, is pursued as a way to grow 2D materials on an industrial scale. Challenges in separating the 2D material from the substrate, in scalability and in homogeneity are the major factors complicating the delivery of applications of the promised ‘miracle’ material graphene in the past 18 years, despite significant efforts.

Chemical vapor deposition (CVD) can be used to grow bulk crystals of most van der Waals materials for exfoliation, but also to grow single layers on metallic substrates. Graphene growth on metals (most notably copper, iridium, and ruthenium) scales very well, but suffers from different rotational domains dominating the electronic properties. On the other hand, epitaxial graphene on silicon carbide, which is grown on the silicon face of SiC by thermal decomposition, has (almost) perfect rotational ordering, although it is harder to separate from its substrate and still exhibits varying electronic properties [6–10].

## 1.2 COMBINING LATTICES: THE FRENKEL-KONTOROVA MODEL

In general, when combining two different lattices, two things can happen. Either both lattices adapt a single shared lattice, the **commensurate** phase, or both lattices retain their own lattice, without significant distortion, known as the **incommensurate** phase. However, a boundary region between these two phases exists in the phase diagram, where lattices partially comply to each other and commensurate regions co-exist with domain boundaries in between, in which all relative lattice strain is contained. As such a (quasi-)periodic pattern of commensurate regions and domain boundaries can form with a periodicity that can be much larger than the underlying periodicities. This new, larger periodicity is called the ‘**superlattice**’, and the resulting pattern is called a **moiré pattern**. The spatial frequency (i.e. the inverse of the lattice constant) of the superlattice is the difference of the spatial frequencies of the constituting lattices. Therefore, the smaller the difference between the lattice constants, the larger the periodicity of the superlattice.

Sometimes it is useful to distinguish higher-order commensurate phases from incommensurate phases. In case of a higher-order commensurate phase, the following holds for the lattice constant  $a_a$  and  $a_b$  of the two lattices:

$$na_a = ma_b$$

where  $n, m$  are (non-equal) integers. For larger integers  $n, m$ , the distinction from (partially) incommensurate becomes increasingly irrelevant, especially in the one-dimensional case.

Whether an incommensurate, commensurate, or mixed state occurs depends on the lattice mismatch, the interlayer interaction (Van der Waals forces) and the interaction within the layer (covalent bonds). This holds true in simple 1D models, in traditional epitaxy, and in van der Waals heterostacks.

The one-dimensional Frenkel-Kontorova (FK) model can be adapted to describe this phase transition between incommensurate and commensurate stacking. In its original, most simple form, the FK-model describes a chain of harmonically interacting particles

subject to a sinusoidal potential. To give an accurate description of the phase transition in a bilayer of one-dimensional atomic chains, two modifications have to be made. First, the sinusoidal potential is replaced by the interlayer potential caused by a second, fixed, strained atomic chain. Second, the harmonic interaction between atoms in the other chain is replaced by a suitably more accurate intralayer interaction [11]. Further extensions to two-dimensional interfaces exist, but to describe the full complexity of the phase diagram, it is necessary to incorporate the full complexity of the system: two lattice constants become two pairs of (2D) lattice *vectors*, and at least parts of the inter- and intralayer interaction functions become two-dimensional.

In the 2D case, the extra freedom given by the extra dimension means that higher-order commensurate structures become more relevant and more common, and they are sometimes known as ‘reconstructions’. They are named after the size and orientation of the unit cell with respect to one lattice, e.g. the reconstruction of graphene on SiC(0001) is denoted  $(6\sqrt{3} \times 6\sqrt{3}) R30^\circ$ , as a unit vector of the full unit cell is given by  $\mathbf{a}' = 6\mathbf{a}_0 + 6\mathbf{a}_1$ , which is  $30^\circ$  rotated with respect to the unit vectors  $\mathbf{a}_0, \mathbf{a}_1$  of the SiC surface. Here,  $|6\mathbf{a}_0 + 6\mathbf{a}_1| = 6\sqrt{3}|\mathbf{a}_0| \approx 13|\mathbf{b}_0|$  where  $|\mathbf{b}_0| = 0.246 \text{ nm}$  is the lattice constant of graphene [12–14]<sup>3</sup>.

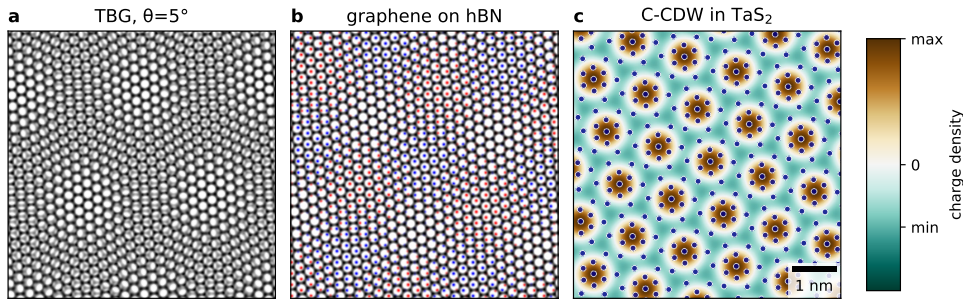


**Figure 1.2: Diagrams of superlattices.** **a**, Twisted bilayer graphene (TBG) with a twist angle  $\theta = 5^\circ$ . **b**, Graphene on hexagonal boron nitride with the same relative twist angle. As a result of the lattice mismatch, the moiré pattern is slightly smaller **c**, The commensurate charge density wave (C-CDW) and the corresponding star-of-David periodic lattice distortion of the tantalum atoms in  $\text{TaS}_2$ , where twelve atoms in the unit cell move slightly towards the charge density center on the thirteenth tantalum atom. The sulfur atoms are omitted for clarity. Scalebar applies to all panels.

Even for the limited case of two hexagonal lattices with similar lattice constants (e.g. graphene-on-hBN, TBG or graphene on biaxially strained graphene), the influence of twist angle, lattice mismatch and a 2D interlayer interaction function mean that in addition to ‘simple’ hexagonal moiré patterns (as shown in Figure 1.2**a,b**), additional stripe phases and spiral domain wall phases can appear [15–19], which are studied in detail in Chapter 7.

<sup>3</sup>Typically one would claim strict equality ( $=$ ) for the reconstruction, not  $\approx$ , but in Chapters 4 and 7 it will become clear that this is inaccurate.

### 1.3 CHARGE DENSITY WAVES

An additional way to combine two lattices in van der Waals materials is to combine the atomic lattice with the lattice of the **Charge Density Waves** (CDWs) occurring in some TMDs. CDWs are the multidimensional equivalent of the classical Peierls transition, where a new periodicity larger than the original atomic periodicity forms spontaneously. In TMDs, typical CDW periodicities include  $3 \times 3$  and  $\sqrt{13} \times \sqrt{13}$ . In this case, the atomic positions over several unit cells and the associated electron density reorder to exchange electronic (band) energy with Coulomb energy of the atomic core positions, as illustrated in Figure 1.2c. The electronic energy is typically lowered by opening a band gap around the Fermi energy, lowering the energy of the states below the Fermi energy. This means the CDW forms only below a critical transition temperature, when the occupancy of the states above the Fermi energy is low enough to actually lower the total energy. It also means CDWs dramatically alter the electronic properties of a material, reducing the conductivity by orders of magnitude as the temperature decreases below the transition temperature.

A particularly complicated example which we will study in this thesis is 1T-TaS<sub>2</sub>, where as the temperature increases, the CDW transitions from insulating commensurate (C-CDW,  $(\sqrt{13} \times \sqrt{13}) R13.9^\circ$ , i.e.  $\mathbf{a}_{\text{CDW}} = 3\mathbf{a}_0 + \mathbf{a}_1$ , the example illustrated in Figure 1.2c) to semiconducting nearly-commensurate (NC-CDW,  $(\sqrt{13} \times \sqrt{13}) R10.9^\circ$ ) to incommensurate (IC-CDW,  $(\sqrt{13} \times \sqrt{13}) R0^\circ$ , i.e.  $\mathbf{a}_{\text{CDW}} = \sqrt{13}\mathbf{a}_0$ ), until it finally disappears.

However, the mechanism behind the Peierls transition does not translate to physical systems in more than one dimension. Although significant progress has been made in recent years to theoretically model and understand real CDW systems (e.g. Ref. [20]), the CDW states in bulk 1T-TaS<sub>2</sub>, in particular the NC-CDW remain not fully understood. Additionally, in the context of 2D materials, the behavior of the CDW in the 2D limit of the material and the possibility to combine it with additional lattices in heterostacks open up new possibilities to modify the CDW behavior and therefore the electronic properties.

### 1.4 STUDYING DOMAINS IN VAN DER WAALS MATERIALS

The existence of different domains and the spatial variability of such domains turn out to be essential to explain the (variation of) electronic properties in heterostructures of van der Waals materials. In particular for van der Waals systems where the lattice mismatch is small, any small variation in the atomic lattice is magnified in the superlattice, which often determines the electronic properties. This means these materials, such as the aforementioned systems of superconducting ‘magic’ angle twisted bilayer graphene and NC-CDW 1T-TaS<sub>2</sub> and even epitaxial graphene on SiC, are extra sensitive to local variations, e.g. a small atomic strain in TBG can break the superconductivity [21]. The best way to study such variations and domains is to directly image them.

Traditionally<sup>4</sup>, Scanning Tunneling Microscopy (STM) (and to a lesser extent Atomic Force Microscopy (AFM)) has been used extensively to study van der Waals materials, their growth and the existence of different (mostly rotational) domains. This technique is very well suited as it is intrinsically surface sensitive and can image the materials with atomic resolution. However, STM imaging is relatively slow. The atomically sharp tip

<sup>4</sup>Insofar ‘traditionally’ is applicable to a field that has existed for only 18 years



needed for STM experiments is fragile and can be easily destroyed by surface contaminations. The surface sensitivity of STM is however so extreme, that distinguishing what is happening in atomic layers beyond the top layer at the surface is hard, if not in most cases impossible. Another technique with atomic resolution, transmission electron microscopy (TEM), has also been used and has its own strengths, but it measures a projection of the sample along the direction of the electron beam. This necessitates extra effort and requirements to the sample to be able to separate the signal originating from the van der Waals material under study from the signal due to the substrate.

## 1.5 CONTENT OF THIS THESIS

In this thesis, we will use Low-Energy Electron Microscopy (LEEM) to study domains in van der Waals heterostructures. LEEM has advantages in studying 2D materials compared to other techniques. Unlike TEM, it reflects electrons off the sample surface at low energies and is therefore inherently surface sensitive and much less prone to damaging the material itself. However, the electrons still penetrate the material to some depth. This enables for example counting the number of graphene layers on top of a substrate and imaging the local stacking of the first few layers of atoms and therefore the stacking domains.

Chapter 2 briefly explains the operating principles and imaging modes of LEEM. However, obtaining the images is only part of the work. To extract the most from the data obtained with a LEEM, it is necessary to properly calibrate the data, correct for sample drift and visualize the resulting multi-dimensional datasets. This process is described in Chapter 3.

In Chapter 4, we use a specific imaging mode called Dark Field LEEM to distinguish the different stackings of bilayer and trilayer graphene. We show that stacking domains are intrinsic to (few-layer) epitaxial graphene on SiC due to the strain exerted by the SiC substrate. This has implications for the process of hydrogen intercalation, which is used to create so-called quasi-free standing graphene. We show that the hydrogen does not penetrate the graphene, except at pre-existing point defects in the graphene, and travels below the graphene, preferentially along the domain boundaries.

Extending on this, Chapter 5 explores how in few-layer graphene, the domain boundaries themselves can be directly imaged using LEEM and we compare the contrast mechanism in twisted bilayer graphene and in the strained graphene on SiC. The imaging of the domain boundaries is applied to twisted bilayer graphene in Chapter 6 to characterize the spatial variations of the moiré pattern, governing the electronic properties of such samples, as well as temporal fluctuations of the moiré lattice. Although these fluctuations correspond to atomic movements of less than 70 pm, which is much smaller than the resolution of the LEEM, they can be imaged using a magnification factor due to the moiré pattern itself. The same magnification enables the imaging of edge dislocations in the atomic lattice. In Chapter 7, the same imaging mechanism is applied to study the morphology of the stacking domains in several different graphene on SiC samples. The morphology of the stacking domains highlights that even in the most homogeneous of such samples, there is an intrinsic strain disorder, caused by a spontaneous symmetry breaking due to both atomic edge dislocations and the coexistence of striped and triangular domains.





In Chapter 8, we change gears and use LEEM to study the superlattices occurring in TaS<sub>2</sub>. This TMD occurs in different polytypes, i.e. different internal arrangements of the atoms within the van der Waals layers. After showing that LEEM can be used to distinguish different stackings of mixes of such polytypes, we study the interaction of the atomic lattice of TaS<sub>2</sub> with the temperature dependent Charge Density Waves occurring in the 1T polytype of TaS<sub>2</sub>.

Finally, a short outlook on the implications of this research and future opportunities is given in Chapter 9.

## REFERENCES

1. M. C. Geisler, J. H. Smet, V. Umansky, et al. Detection of a Landau Band-Coupling-Induced Rearrangement of the Hofstadter Butterfly. *Physical Review Letters* **92**, 256801. doi:[10.1103/PhysRevLett.92.256801](https://doi.org/10.1103/PhysRevLett.92.256801) (2004).
2. K. S. Novoselov, A. K. Geim, S. V. Morozov, et al. Electric Field Effect in Atomically Thin Carbon Films. *Science* **306**, 666–669. doi:[10.1126/science.1102896](https://doi.org/10.1126/science.1102896) (2004).
3. M. Ates, E. Yilmaz & M. K. Tanaydın. In *Chalcogenide-Based Nanomaterials as Photocatalysts* (ed M. M. Khan) 307–337 (Elsevier, 2021). doi:[10.1016/B978-0-12-820498-6.00014-7](https://doi.org/10.1016/B978-0-12-820498-6.00014-7).
4. Y. Cao, V. Fatemi, S. Fang, et al. Unconventional superconductivity in magic-angle graphene superlattices. *Nature* **556**, 43–50. doi:[10.1038/nature26160](https://doi.org/10.1038/nature26160) (2018).
5. S. Lisi\*, X. Lu\*, T. Benschop\*, T. A. de Jong\*, et al. Observation of flat bands in twisted bilayer graphene. *Nature Physics* **17**, 189–193. doi:[10.1038/s41567-020-01041-x](https://doi.org/10.1038/s41567-020-01041-x) (2021).
6. J. Kautz, J. Jobst, C. Sorger, et al. Low-Energy Electron Potentiometry: Contactless Imaging of Charge Transport on the Nanoscale. *Scientific Reports* **5**, 13604. doi:[10.1038/srep13604](https://doi.org/10.1038/srep13604) (2015).
7. S.-H. Ji, J. B. Hannon, R. M. Tromp, et al. Atomic-scale transport in epitaxial graphene. *Nature Materials* **11**, 114–119. doi:[10.1038/nmat3170](https://doi.org/10.1038/nmat3170) (2012).
8. F. Kisslinger, C. Ott, C. Heide, et al. Linear magnetoresistance in mosaic-like bilayer graphene. *Nature Physics* **11**, 650–653. doi:[10.1038/nphys3368](https://doi.org/10.1038/nphys3368) (2015).
9. M. K. Yakes, D. Gunlycke, J. L. Tedesco, et al. Conductance Anisotropy in Epitaxial Graphene Sheets Generated by Substrate Interactions. *Nano Letters* **10**, 1559–1562. doi:[10.1021/nl9035302](https://doi.org/10.1021/nl9035302) (2010).
10. D. Momeni Pakdehi, J. Aprojanz, A. Sinterhauf, et al. Minimum Resistance Anisotropy of Epitaxial Graphene on SiC. *ACS Applied Materials & Interfaces* **10**, 6039–6045. doi:[10.1021/acsami.7b18641](https://doi.org/10.1021/acsami.7b18641) (2018).
11. A. M. Popov, I. V. Lebedeva, A. A. Knizhnik, Y. E. Lozovik & B. V. Potapkin. Commensurate-incommensurate phase transition in bilayer graphene. *Physical Review B* **84**, 045404. doi:[10.1103/PhysRevB.84.045404](https://doi.org/10.1103/PhysRevB.84.045404) (2011).



12. C. Riedl, U. Starke, J. Bernhardt, M. Franke & K. Heinz. Structural properties of the graphene-SiC(0001) interface as a key for the preparation of homogeneous large-terrace graphene surfaces. *Physical Review B* **76**, 245406. doi:[10.1103/PhysRevB.76.245406](https://doi.org/10.1103/PhysRevB.76.245406) (2007).
13. S. Kim, J. Ihm, H. J. Choi & Y.-W. Son. Origin of Anomalous Electronic Structures of Epitaxial Graphene on Silicon Carbide. *Physical Review Letters* **100**, 176802. doi:[10.1103/PhysRevLett.100.176802](https://doi.org/10.1103/PhysRevLett.100.176802) (2008).
14. F. Varchon, P. Mallet, J.-Y. Veuillen & L. Magaud. Ripples in epitaxial graphene on the Si-terminated SiC(0001) surface. *Physical Review B* **77**, 235412. doi:[10.1103/PhysRevB.77.235412](https://doi.org/10.1103/PhysRevB.77.235412) (2008).
15. I. V. Lebedeva, A. V. Lebedev, A. M. Popov & A. A. Knizhnik. Dislocations in stacking and commensurate-incommensurate phase transition in bilayer graphene and hexagonal boron nitride. *Physical Review B* **93**, 235414. doi:[10.1103/PhysRevB.93.235414](https://doi.org/10.1103/PhysRevB.93.235414) (2016).
16. S. Quan, L. He & Y. Ni. Tunable mosaic structures in van der Waals layered materials. *Physical Chemistry Chemical Physics* **20**, 25428–25436. doi:[10.1039/C8CP04360D](https://doi.org/10.1039/C8CP04360D) (2018).
17. J. Ravník, I. Vaskivskiy, Y. Gerasimenko, et al. Strain-Induced Metastable Topological Networks in Laser-Fabricated TaS<sub>2</sub> Polytype Heterostructures for Nanoscale Devices. *ACS Applied Nano Materials* **2**, 3743–3751. doi:[10.1021/acsanm.9b00644](https://doi.org/10.1021/acsanm.9b00644) (2019).
18. C. Gutiérrez, C.-J. Kim, L. Brown, et al. Imaging chiral symmetry breaking from Kekulé bond order in graphene. *Nature Physics* **12**, 950–958. doi:[10.1038/nphys3776](https://doi.org/10.1038/nphys3776) (2016).
19. I. V. Lebedeva & A. M. Popov. Two Phases with Different Domain Wall Networks and a Reentrant Phase Transition in Bilayer Graphene under Strain. *Physical Review Letters* **124**, 116101. doi:[10.1103/PhysRevLett.124.116101](https://doi.org/10.1103/PhysRevLett.124.116101) (2020).
20. J. Henke, F. Flicker, J. Laverock & J. van Wezel. Charge order from structured coupling in VSe<sub>2</sub>. *SciPost Physics* **9**, 056. doi:[10.21468/SciPostPhys.9.4.056](https://doi.org/10.21468/SciPostPhys.9.4.056) (2020).
21. F. Mesple, A. Missaoui, T. Cea, et al. Heterostrain Determines Flat Bands in Magic-Angle Twisted Graphene Layers. *Physical Review Letters* **127**, 126405. doi:[10.1103/PhysRevLett.127.126405](https://doi.org/10.1103/PhysRevLett.127.126405) (2021).

